Synthesis and Properties of Novel Highly Fluorescent Pyrrolopyridazine Derivatives

Teruyuki Mitsumori, Michael Bendikov, Josep Sedó, and Fred Wudl*

Department of Chemistry and Biochemistry, Exotic Materials Institute, University of California, Los Angeles, California 90095-1569

Received February 11, 2003. Revised Manuscript Received July 9, 2003

We report here the synthesis, X-ray structures, optical and electrochemical properties, and density functional calculations for new pyrrolopyridazine derivatives. Ten strongly luminescent heterocycles were synthesized by 1,3-dipolar cycloaddition reactions between alkylated pyridazine or cinnoline and naphthoquinone or dimethyl acetylenedicarboxylate (**DMAD**). They are benzo[*f*]pyridazino[6,1-*a*]isoindole-5,10-diones (**BPID**) **1**−**4**, benzo[*f*]-pyridazino[6,1-*a*]isoindole (**BPI**) **5**, pyrrolo[1,2-*b*]cinnolines (**PC**) **6** and **7**, and pyrrolo[1,2-*b*]pyridazines (**PP**) **8**−**10**. The relative luminescence quantum yield can be as high as 90% and the heterocycles are luminescent in the solid state, which indicates that there is little self-quenching in these systems. Furthermore, we have shown that the optical properties of pyrrolopyridazines can be tuned by substitutions in different ring positions. An unexpected blue shift and a large red shift with a different π conjugation system were explained by aromaticity arguments using DFT calculations and X-ray crystal structures. Electrochemical investigation has shown that the redo potentials of the new heterocycles could be controlled by design. The synthesis of a series of compounds allowed detailed analysis of substituent effects on structures, frontier orbitals, and luminescent and electrochemical properties.

Introduction

Light-emitting organic compounds (organic luminophors) continue to arouse strong interest because of their fascinating applications such as electroluminescent materials, sensors, lasers, and other semiconductor devices.[1,2] Two types of organic materials, small molecules and polymers, are commonly used for organic thin-film device fabrication. Small molecules have the advantages of facile emission color control and ease of fabrication of multilayer devices. They, however, still have stability problems and rules governing the correlation between structure and fluorescence efficiency are still in their infancy.[3]

While many chromophores have been designed and synthesized,[4,5] it is still essential to find molecules which exhibit high fluorescence, little self-quenching, proper energy levels, pure RGB color, and high stability. Therefore, strategies for tuning colors and controlling energy levels without reducing fluorescence are very important. Recently, our group reported a series of highly blue fluorescent pyrrolopyridazines.[6] Since then, our group has realized that it is imperative to investigate the possibility of tuning colors and energy levels by modifying the structures of these luminophors.

Here, we report complete characterization of new pyrrolopyridazines that exhibit highly efficient blue and green fluorescence. We have successfully obtained 10 new compounds (**1**−**10**) with different HOMO and LUMO levels and consequently different emission colors (Figure 1). Such a strategy for design provides feasible ways to new emissive chromophores. Three compounds were characterized by X-ray structure analysis. The structural data, combined with density functional calculations, allowed for a better understanding of the pyrrolopyridazine chromophore.

Results and Discussion

Synthesis. New organic compounds reported in this paper are presented in Figure 1. Strategies for the

* To whom correspondence should be addressed. E-mail: wudl@chem.ucla.edu.

(1) (a) Tullo, A. H. *Chem. Eng. News* **2000**, *78*, 25. (b) Tang, C. W.; Van Slyke, S. A. *Appl. Phys. Lett.* **1987**, *51*, 913. (c) Woo, H. S.; Czerw, R.; Webster, S.; Carroll, D. L.; Ballato, J.; Strevens, A. E.; O'Brien, D.; Blau, W. *J. Appl. Phys. Lett.* **2000**, *77*, 1393. (d) Chen, L.; McBranch, D. W.; Wang, H.-L.; Helgeson, R.; Wudl, F.; Whitten, D. C. *Proc. Natl. Acad. Sci. U.S.A.* **1999**, *96*, 12287. (e) Hide, F.; Díaz-García, M. A.; Schwartz, B. J.; Andersson, M.; Pei, Q.; Heeger, A. J. *Science* **1996**, *273*, 1833. (f) Swager, T. M. *Acc. Chem. Res.* **1998**, *31*, 201. (g) Pei, Q.; Yu, G.; Zhang, C.; Yang, Y.; Heeger, A. J. *Science* **1995**, *269*, 1086.

(2) (a) Tang, C. W.; VanSlyke, S. A.; Chen, C. H. *J. Appl. Phys.* **1989**, 3610. (b) Burroughes, J. H.; Bradley, D. D. C.; Brown, A. R.; Marks, R. N.; Mackay, K.; Friend, R. H.; Burns, P. L.; Holmes, A. B. *Nature* **1990**, *347*, 539. (c) Braun, D.; Heeger, A. J. *Appl. Phys. Lett.* **1991**, *58*, 1982. (d) Kepler, R. G.; Beeson, P. M.; Jacobs, S. J.; Anderson, R. A.; Sinclair, M. B.; Valencia, V. S.; Cahill, P. A. *Appl. Phys. Lett.* **1995**, *66*, 3618. (e) Thompson, M. A.; Forrest, S. R. *Nature* **2000**, *403*, 750. (f) Srdanov, G.; Wudl, F. U.S. Patent 5,189,136, 1993. (g) Lee, S. H.; Nakamura, T.; Tsutsui, T. *Org. Lett.* **2001**, *3*, 2006. (h) Noda, T.; Shirota, Y. *J. Am. Chem. Soc.* **1998**, *120*, 971 (i) Sheats, J. R.; Antoniadis, H.; Hueschen, M.; Leonard, W.; Miller, J.; Moon, R.; Roitman, D.; Stocking, A. *Science* **1996**, *273*, 884. (j) Goldfinger, M. B.; Crawford, K. B.; Swager, T. M. *J. Am. Chem. Soc.* **1997**, *119*, 4578. (k) Neef, C. J.; Ferraris, J. P. *Macromolecules* **2000**, *33*, 2311. (l) Pei, Q.; Yang, Y. *J. Am. Chem. Soc.* **1996**, *118*, 7416.

(3) (a) Willardson, R. K.; Weber, E.; Mueller, G.; Sato, Y. *Electroluminescence I, Semiconductors and Semimetals Series*; Academic Press: New York, 1999. (b) Bulovic, V.; Forrest, S. R.; Mueller-Mach, R.; Mueller, G. O.; Leslela, M.; Li, W.; Ritala, M.; Neyts, K. *Electroluminescence II Semiconductors and Semimetals Series*; Academic Press: New York, 2000.

(4) Chen, C. H.; Shi, J. *Coord. Chem. Rev.* **1998**, *171*, 161.

(5) Kido, J.; Okamoto, Y. *Chem. Rev.* **2002**, *102*, 2357.

(6) Cheng, Y.; Ma, B.; Wudl, F. *J. Mater. Chem.* **1999**, *9*, 2183.

10.1021/cm0340532 CCC: $25.00
Published on Web 08/29/2003

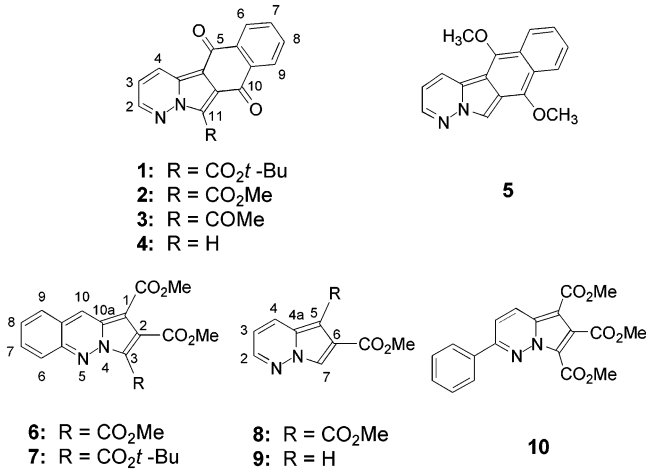

Figure 1. Structures of the molecules reported in this paper.

pyrrolopyridazine syntheses are depicted in Schemes 1−3.

The preparation of benzo[*f*]pyridazino[6,1-*a*]isoindole-5,10-dione (**BPID**) derivatives **1**−**3** was carried out in two steps using the methodology described in ref 7 (Scheme 1). Initially, *N*-alkylations of pyridazine afforded pyridazinium salts. Rapid cycloadditions occurred when pyridazinium salts were allowed to react with naphthoquinone in the presence of triethylamine to give **1**−**3**. Dehydrogenation after cycloaddition had occurred with air, without adding any oxidizing agent. Decarboxylation of a carboxyl group[8] in the 11-position occurred smoothly using hydroiodic acid in acetone to produce the desired dione **4** (Scheme 1). Interestingly, decarboxylation[9] occurred starting from both **1** and **3**. Dione **4** was reduced by a metal ketyl[10] to the benzo[*f*]-pyridazino[6,1-*a*]isoindole (**BPI**) **5** (Scheme 1). Compound **5** is slightly sensitive to light and oxygen but the solid could be stored for about 1 month without decomposition under argon at −15 °C.

Compounds **PC**(**6**) and **PP**(**10**) were prepared in one step[8] as described in Schemes 2 and 3. Cinnoline was allowed to react with dimethyl acetylenedicarboxylate (**DMAD**) directly in methanol at low temperature (0 °C) to afford the product **6**. 3-Phenylpyridazine was prepared according to the literature[11] and was allowed to react with **DMAD** at room temperature to afford **10**.

Preparation of **PC** (**7**) was carried out in two steps using a similar method[7] as for **BPID** (**1**) (Scheme 2). *N*-Alkylation of cinnoline with *tert*-butyl bromoacetate afforded a mixture of 1- and 2-substituted cinnoline salts. The 2-substituted cinnoline salt **S4** (from the crude reaction mixture) was allowed to react with **DMAD** to afford **7**.

Pyrrolopyridazine triester **11** was prepared by the method reported previously[6] and was selectively decarboxylated under appropriate conditions[12,13] (Scheme 3) to afford **8** and **9**.

Optical Properties. The absorption and fluorescence spectra of compounds **1**−**10** were recorded in DMSO, methanol, methylene chloride, and hexane solution at room temperature.[14] Relative quantum yields were determined by using 9,10-diphenylanthracene in de-

Scheme 1. Synthetic Routes to 1−5

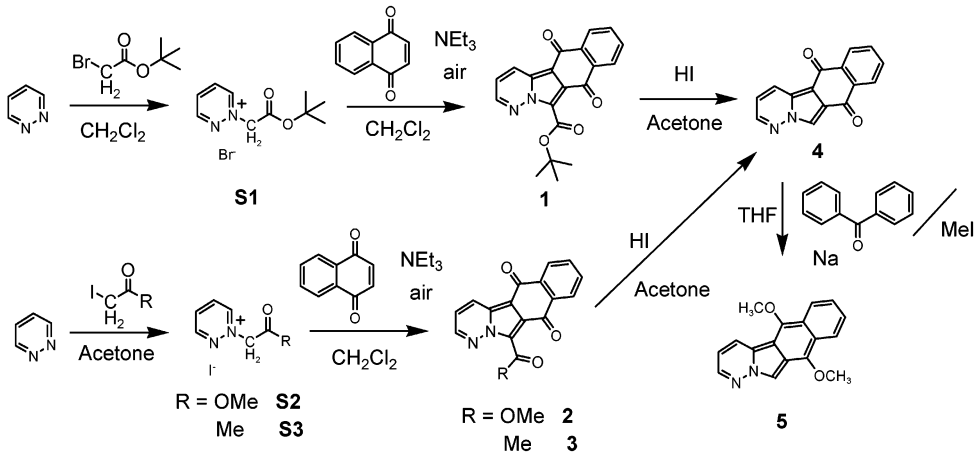

Scheme 2. Synthetic Routes to 6 and 7

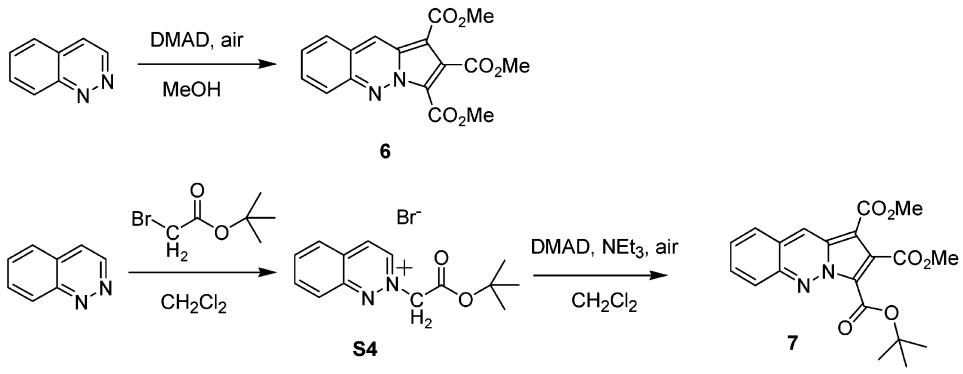

Table 1. λ_{max} (nm) of Absorption Spectra, λ_{max} (nm) of Fluorescence Spectra, and Relative Quantum Efficiency (%) of Compound 1−10

	absorption (λ_{max}/nm)				fluorescence (λ_{max}/nm) (quantum efficiency (%))			
compd	DMSO	MeOH	CH_2Cl_2	hexane	DMSO	MeOH	CH_2Cl_2	hexane
1	421	417	421	419	529 (14)	525 (21)	498 (5)	475 (0.4)
2	420	*a*	420	*a*	515 (9)	*a*	495 (2)	*a*
3	421	422	424	423	541 (2)	535 (0.8)	501 (0.5)	475 (0.1)
4	426	*a*	425	*a*	528 (46)	*a*	501 (40)	*a*
5	381	381	384	385	458 (85)	445 (73)	445 (82)	435 (39)
6	437	435	440	448	526 (67)	519 (83)	522 (82)	519 (79)
7	439	438	442	449	530 (58)	524 (66)	529 (65)	524 (66)
8	369	369	369	369	449 (92)	445 (77)	441 (81)	431 (89)
9	370	369	370	371	462 (73)	463 (63)	455 (74)	442 (67)
10	348	346	350	351	446 (81)	443 (73)	444 (68)	442 (75)

[a] Insoluble.

Scheme 3. Synthetic Routes to 8−10

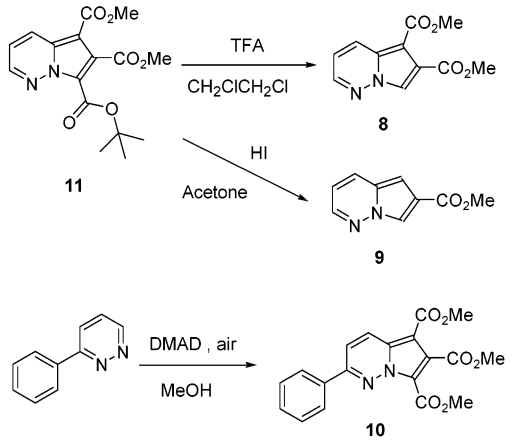

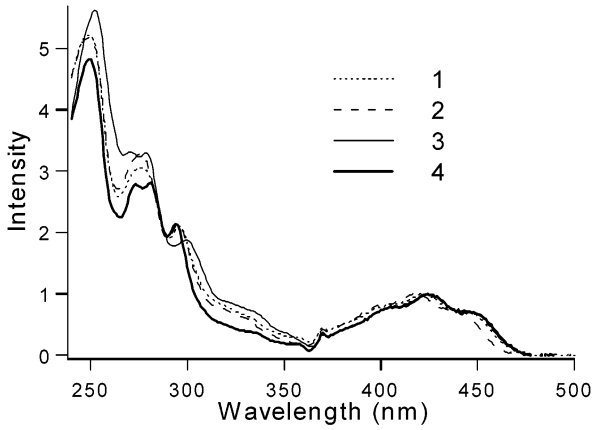

Figure 2. Normalized absorption spectra of compounds **1**−**4** in dichloromethane.

gassed hexane ($\Phi = 0.96$)[6] and perylene in degassed cyclohexane ($\Phi = 0.94$)[15] as reference. 9,10-Diphenylanthracene was used for compounds (**5** and **8**−**10**), which emit blue light, and perylene was used for compounds (**1**−**4**, **6**, and **7**), which are green emitters. As shown in Table 1, **BPI** (**5**) and **PPs** (**8**−**10**) are very intense blue emitters (λ_{max} of fluorescence around 435−460 nm) and **PCs** (**6**, **7**) are very intense green emitters (λ_{max} of fluorescence around 520 nm). Their quantum efficiencies reach up to 92%.

While the **BPIDs 1**−**4** had lower quantum efficiencies (<46%), their emissions showed strong solvent dependence. In a highly polar solvent, such as DMSO, their fluorescences were the most red-shifted but the absorbances did not change with solvent polarity. Consequently, the Stokes shifts of the compounds in polar DMSO reached 100 nm. This indicates that the Franck−Condon states do not change significantly but the equilibrium states (after Franck−Condon states) depend on the environment.[15,16] We would expect some significant change in conformation and solvation in excited states.[17,18] As for quantum efficiency, polar solvents also provide the highest values. To avoid internal conversion, it is required to stabilize the dipole orientations in the excited states; that is, polar environments are preferred.

Interestingly, contrary to **BPIDs**, the absorption of **PCs** (**6**,**7**) showed a blue shift in polar solvents (by 10 nm) and their fluorescences showed only minor differences among various solvents. This indicates the energy of the Franck−Condon states increased in polar solvents because the solvation energy might have a negative term.[15] It also implies that excited **PCs** are less polar especially in polar solvents.[18]

The absorption and fluorescence spectra of **BPIDs** (**1**−**4**) are shown in Figures 2 and 3. Compared with **BPIDs** (**1**−**3**), **BPID** (**4**) shows slightly red-shifted spectra, but obviously the profiles of the optical spectra are very similar. This indicates that substituents at the 11-position in **BPIDs** exert little influence on the optical spectra. Yet, unexpectedly, the quantum efficiencies of **4** (46% in DMSO) are much higher than those of **1**−**3**

(7) Farum, D. G.; Alamo, R. J.; Dunston, J. M. *J. Org. Chem*. **1967**, *32*, 1130.
(8) Letsinger, R. L.; Lasco, R. *J. Org. Chem*. **1956**, *21*, 764.
(9) Bobrovskii, S. I.; Lushnikov, S. I.; Bundel, Y. G. *Zh. Org. Khim*. **1989**, *25*, 2241.
(10) Seki, H.; Hoshino, M.; Kounose, S. *J. Chem. Soc., Faraday Trans*. **1996**, *92*, 2579.
(11) (a) Strekovski, L.; Wilson, D.; Mokrosz, J. L.; Mokrosz, M. J.; Harden, D. B.; Tanious, F. A.; Wydra, R. L.; Crow, S. A. *J. Med. Chem*. **1991**, *34*, 580 (b) Wilson, W. D.; Strekowski, L.; Tanious, F. A.; Watson, R. A.; Mokrosz, J. L.; Strekowska, A.; Webster, G. D.; Neidle, S. *J. Am. Chem. Soc*. **1988**, *110*, 8292.
(12) Keumi, T.; Morita, T.; Inui, Y.; Teshima, N.; Kitajima, H. *Synthesis* **1985**, 979.
(13) Ito, S.; Uno, H.; Murashima, T.; Ono, N. *Tetrahedron Lett*. **2001**, *42*, 45.
(14) Sharma, A.; Schulman, S. G. *Fluorescence Spectroscopy*; John Wiely & Sons: New York, 1999.
(15) Berman, I. *Handbook of Fluorescence Spectra of Aromatic Molecules*; Academic Press: New York, 1965.
(16) Based on second order-perturbation theory,[17] the differences of dipole moments and polarizabilities between the ground states and the excited states do not change by solvents but diversity of the dipole orientation in the excited states is not negligible.[18]
(17) McRae, E. *J. Phys. Chem*. **1957**, *61*, 562.
(18) Becker, R. S. *Theory and Interpretations of Fluorescence and Phosphorescence*; John Wiley & Sons: New York, 1969.

Table 2. Absorption and Emission Properties of PPH, PPY, and PC (6) in Hexane

Compounds	PPH 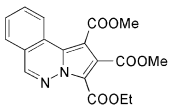	PPY 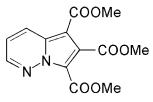	PC (6) 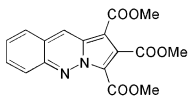
UV-Vis λ max (nm)	319 [a)]	346 [a)]	440
Fluorescence λ max (nm)	432 [a)]	429 [a)]	519
Fluorescence quantum efficiency(%)	7.4 [a)]	84 [a)]	79

[a] Data from ref 6.

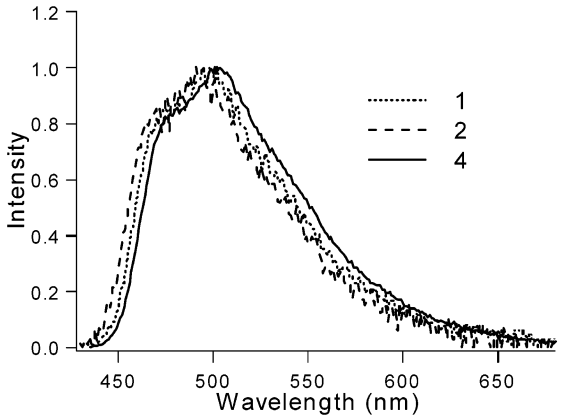

Figure 3. Normalized fluorescence spectra of compounds **1**, **2**, and **4** in dichloromethane.

(14, 9, and 2% respectively, in DMSO). These results led us to conclude that the 11-position plays an important role for the deactivation process in **BPIDs**.

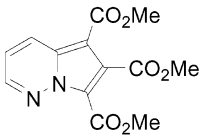

PPY

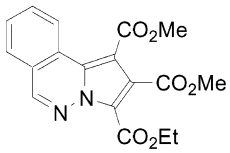

PPH

Examination of the optical spectra of compounds **4**−**7** (Table 1) and pyrrolo[1,2-b]pyridazine-5,6,7-tricarboxylic acid trimethyl ester (**PPY**)[19] reveals that apparently the first absorption bands and the fluorescence spectra of **BPI** (**5**) (absorption ∼ 380 nm; fluorescence = 435−460 nm), **BPIDs** (**1**−**4**) (absorption ∼ 420 nm; fluorescence = 495−530 nm), and **PCs** (**6**, **7**) (absorption ∼ 440 nm; fluorescence = 520−530 nm) are red-shifted compared with **PPY** (absorption ∼ 340 nm; fluorescence ∼ 430 nm), as expected from a longer π-conjugation system. **PCs** (**6**, **7**) are the most red-shifted, but have almost identical spectra, indicating that, not surprisingly, optical spectra are independent of the ester alkyl groups as observed with pyrrolopyridazine.[6] Compared with **BPID** (**4**), the spectra of **BPI** (**5**) are shifted to shorter wavelength and the fluorescence quantum efficiencies increased.

In summary, we can conclude that expansions of the π system in the direction of positions 2 and 3 or 5 and 6 should be a good design strategy in pyrrolopyridazines to obtain highly fluorescent compounds.

Further examination of Table 1 reveals that the absorption and fluorescence spectra of compound **10** show slightly red-shifted spectra (absorption 350 nm; fluorescence 444 nm in CH_2Cl_2), compared with **PPY** (absorption 334 nm; fluorescence 434 nm in CH_2Cl_2). Interestingly, **10** still exhibits high fluorescence efficiency from 70 to 80%, after expanding the π-system by a phenyl group. That is, the π-system can be expanded without reducing quantum efficiency not only by a fused system but also by a phenyl substitution in the proper positions.

As the number of esters decreased from three esters in **PPY**, to two esters in **8**, and further to one ester in **9**, the optical spectra shifted to longer wavelength (fluorescence: 434, 441, and 455 nm, respectively), while quantum efficiency remained high (from 70 to 90%), which indicates that electron-withdrawing ester groups increase the HOMO−LUMO gap slightly but do not reduce fluorescence.

The optical properties of **PPH**, **PPY**, and **PC** (**6**) in hexane are given in Table 2. Previously, we reported that **PPH** showed a blue shift and its quantum efficiency (7.4%) decreased dramatically compared with that of **PPY** (84%).[6] This blue shift of **PPH** is very unusual because, in general, compounds show a red shift upon extension of π conjugation.[20] Compound **PC** (**6**), on the other hand, shows a very large red shift by about 100 nm, and its fluorescence intensity (79%) is still high.

Why does **PPH** exhibit a blue shift compared to **PPY**, while **PPH** has a longer π-conjugated system? Why does **PC** (**6**) exhibit a large red shift simply with a different fused position? We sought to answer the questions using X-ray crystal structures and calculations.

(19) **PPY** was prepared according to the literature procedures.[6]

(20) Silverstein, R. M.; Bassler, G. C. Morrill, T. C. *Spectrometric Identification of Organic Compounds*; John Wiley & Sons: New York, 1981.

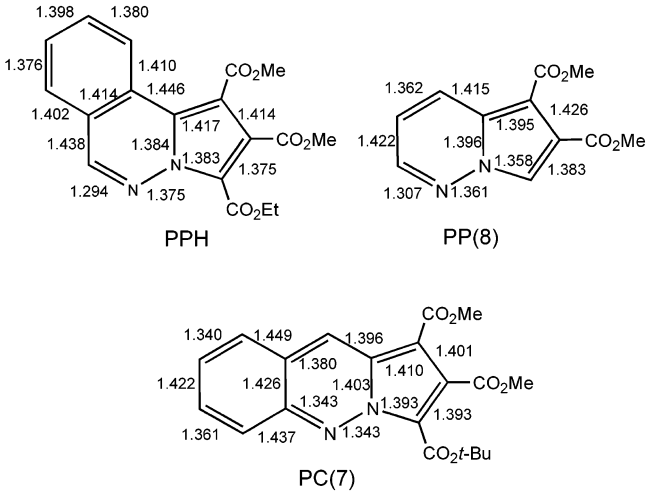

Figure 4. Bond lengths of **PPH**, **PP**, and **PC** from X-ray structures.

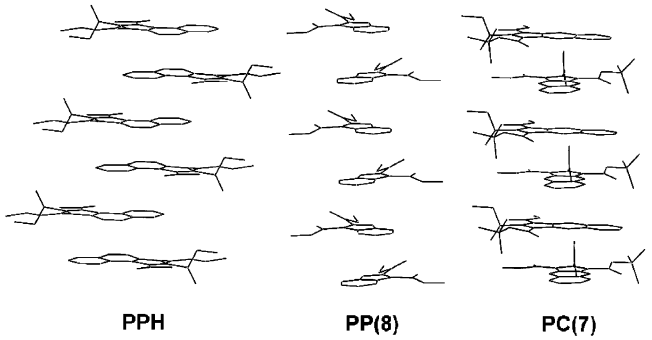

Figure 5. π-Stacking diagrams of **PPH**, **PP** (**8**), and **PC** (**7**).

X-ray Crystal Structures. Single crystals of **PPH**,[21] **PP** (**8**), and **PC** (**7**) were grown from CH_2Cl_2/hexane solution and characterized using X-ray crystallography. To the best of our knowledge, only one X-ray structure of a substituted pyrrolopyridazine derivative (having ring arrangements as in **PC**) was reported previously.[22] Thus, we report the first X-ray crystal structures for heterocycles such as **PPH** and **PP**. Expectedly, the pyrrolopyridazine unit is planar in both systems, supporting the notion that these heterocycles are aromatic.

Figure 4 shows geometries of the heterocycles. Surprisingly, the geometry of the pyrrolopyridazine unit in PPH and PC is significantly different. Thus, the N−N bond length is equal to 1.375 Å in **PPH**, while it is much shorter (1.343 Å) in PC. The N═C bond length in **PPH** (1.294 Å) is significantly shorter than the N═C bond length in PC (1.343 Å). Benzannulation increases aromaticity of the pyrrolopyridazine unit in **PC**, which is evidenced by increased bond equalization.[23] The reasons for differences in X-ray geometries of **PPH** and PC will be discussed later in this paper.

Figure 5 shows the π stacking of **PPH**, **PP** (**8**), and **PC** (**7**). The molecules stack along the *c* axis in **PPH** and **PP** (**8**) and the *a* axis in **PC** (**7**) to form columnar structures. The strong π-stacking interactions are reflected in the distances between π planes: 3.39 Å in **PPH**, 3.34 Å in **PP** (**8**), and 3.31 Å in **PC** (**7**). These values are almost the same as, or smaller than, that of the interplanar distance of graphite (3.35 Å).[24] These π-stacking systems appear strong enough so that these heterocycles are expected to be useful for applications that need high mobility, such as FET devices.[25]

Computational Study of Pyrrolopyridazines. We have performed quantum mechanical density functional calculations[26] at the B3LYP/6-31G(d) level of theory.[27,28] The optimized structures of unsubstituted **PPH**, **PP**, and **PC** (**PPH′**, **PP′**, and **PC′**), Figure 6, were found to be planar by frequency analysis.[29,30] The parent pyrrolopyridazine (**PP′**) is a 10π aromatic system with its N−N bond (1.354 Å) being only slightly longer than that in pyridazine **12** (1.350 Å) and the N═C bond (1.312 Å) being longer than that in pyridazine **12** (1.300 Å).[30] The C(4a)═C(5), C(6)═C(7) double bonds (1.394 and 1.390 Å) are longer than the C(2)−C(3) bond in *N*-methylpyrrole (1.379 Å) and the C(5)−C(6) bond (1.409 Å) is shorter than the C(3)−C(4) bond in *N*-methylpyrrole (1.424 Å). Calculated structure **PP′** shows more delocalization than pyridazine **12** and *N*-methylpyrrole.

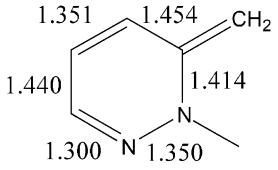

12

Modification of **PP′** by benzannulation in the 2,3-positions produces **PC′** (its analogue, **PC** exhibits a

(21) **PPH** was prepared according to the literature procedures.[6]

(22) Flitsch, W.; Lauterwein, J.; Leimkuehler, M. Leaver, D.; Lewinski, U.; Mattes, R.; Temme, R.; Wibbeling, B. *Liebigs Ann. Chem.* **1990**, *7*, 627.

(23) The standard deviation of the bond lengths in **PP** is 0.037 Å, the standard deviation of the bond lengths (pyrrolopyridazine unit) in **PPH** is 0.043 Å, and that (pyrrolopyridazine unit) in **PC** is only 0.027 Å.

(24) Chung, D. D. L. *J. Mater. Sci.* **2002**, *37*, 1475.

(25) (a) Dimitrakopoulos, C. D.; Mascaro, D. J. *IBM J. Res. Dev.* **2001**, *45*, 11. (b) Dimitrakopoulos, C. D.; Malenfant, P. R. L. *Adv. Mater.* **2002**, *14*, 99. (c) Bredas, J. L.; Calbert, J. P.; Filho, D.A. S.; Cornil, J. *Proc. Natl. Acad. Sci. U.S.A.* **2002**, *99*, 5804. (d) Afzali, A.; Dimitrakopoulos, C. D.; Breen, T. L. *J. Am. Chem. Soc.* **2002**, *124*, 8812. (e) Anthony, J. E.; Broks, J. S.; Eaton, D. L.; Parkin, S. R. *J. Am. Chem. Soc.* **2001**, *123*, 9482. (f) Bredas, J. L.; Beljonne, D.; Cornil, J.; Calbert, J. P.; Shuai, A.; Silbey, R. *Synth. Met.* **2002**, *125*, 107. (g) Anthony, J. E.; Eaton, D. L.; Parkin, S. R. *Org. Lett.* **2002**, *4*, 15. (h) Gruhn, N. E.; Filho, D. A. S.; Bill, T. G.; Malagoli, M.; Coropceanu, V.; Kahn, A.; Bredas, J. L. *J. Am. Chem. Soc.* **2002**, *124*, 7918. (i) Malagoli, M.; Bredas, J. L. *Chem. Phys. Lett.* **2000,** *327*, 13.

(26) (a) Parr, R. G.; Yang, W. *Density-Functional Theory of Atoms and Molecules*; Oxford University Press: New York, 1989. (b) Koch, W.; Holthausen M. C. *A Chemist's guide to density functional theory*; Wiley-VCH: Weinheim, 2000.

(27) (a) Lee, C.; Yang W.; Parr, R. G. *Phys. Rev. B* **1988**, *37*, 785. (b) Becke, A. D. *J. Chem. Phys.* **1993**, *98*, 5648.

(28) All calculations used the GAUSSIAN 98 series of programs. Frisch, M. J.; Trucks, G. W.; Schlegel, H. B.; Scuseria, G. E.; Robb, M. A.; Cheeseman, J. R.; Zakrzewski, V. G.; Montgomery, J. A., Jr.; Stratmann, R. E.; Burant, J. C.; Dapprich, S.; Millam, J. M.; Daniels, A. D.; Kudin, K. N.; Strain, M. C.; Farkas, O.; Tomasi, J.; Barone, V.; Cossi, M.; Cammi, R.; Mennucci, B.; Pomelli, C.; Adamo, C.; Clifford, S.; Ochterski, J.; Petersson, G. A.; Ayala, P. Y.; Cui, Q.; Morokuma, K.; Rega, N.; Salvador, P.; Dannenberg, J. J.; Malick, D. K.; Rabuck, A. D.; Raghavachari, K.; Foresman, J. B.; Cioslowski, J.; Ortiz, J. V.; Baboul, A. G.; Stefanov, B. B.; Liu, G.; Liashenko, A.; Piskorz, P.; Komaromi, I.; Gomperts, R.; Martin, R. L.; Fox, D. J.; Keith, T.; Al-Laham, M. A.; Peng, C. Y.; Nanayakkara, A.; Challacombe, M.; Gill, P. M. W.; Johnson, B.; Chen, W.; Wong, M. W.; Andres, J. L.; Gonzalez, C.; Head-Gordon, M.; Replogle, E. S.; Pople, J. A. A.11.4; Gaussian, Inc.: Pittsburgh, PA, 2002.

(29) We will discuss results of calculations since they were performed on parent systems and do not include any substituent effect except of fused benzene rings.

(30) We note that trends in bond length are very similar in crystal structures, except for the small substituent effect, mostly on the N−C bond of the five-membered ring.

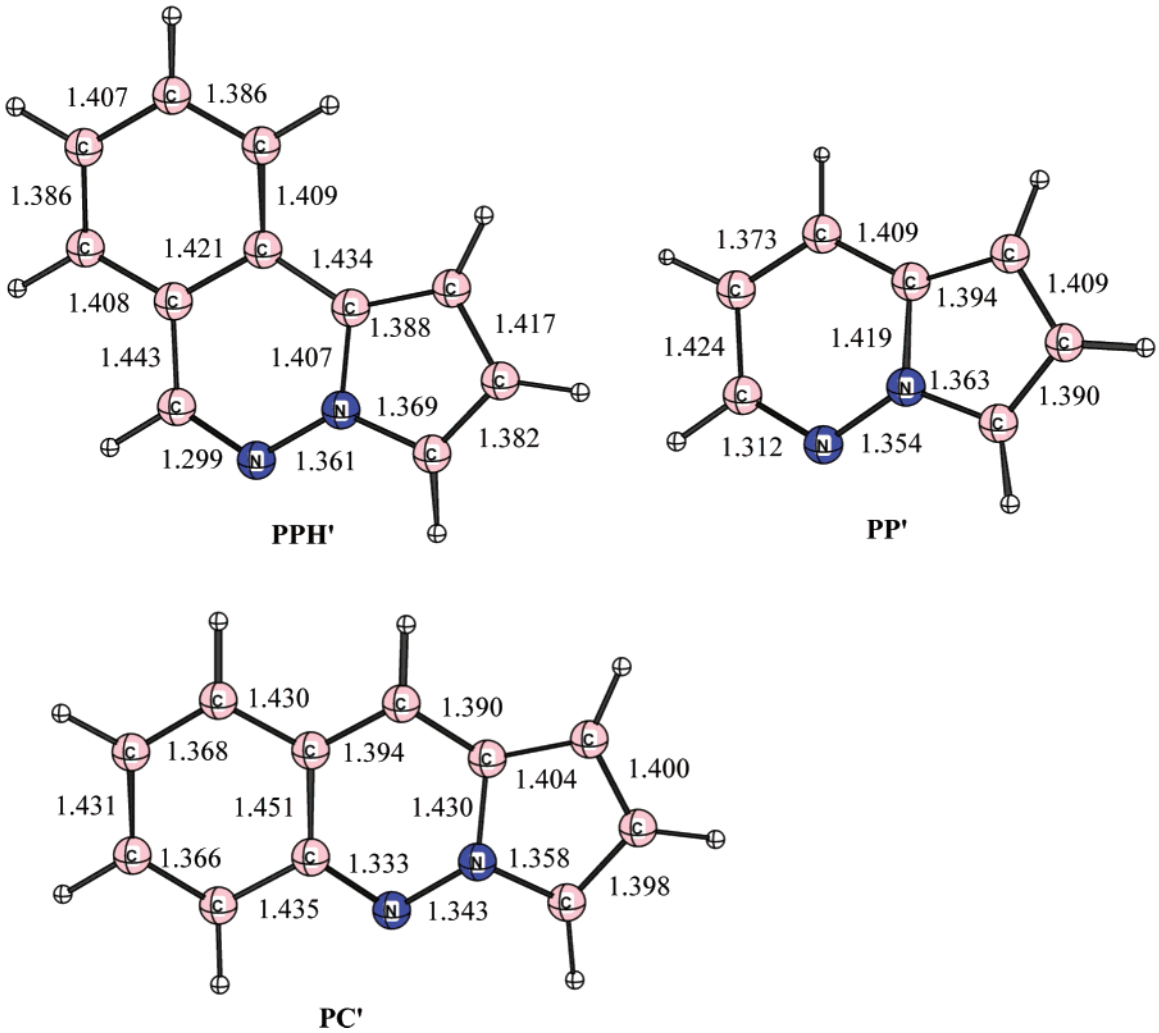

Figure 6. Optimized structures (B3LYP/6-31G(d)) of **PPH′**, **PP′**, and **PC′**.

longer wavelength absorption, 440 nm, compared to **PP**, 346 nm, Table 2). An analysis of calculated geometries[30] (Figure 6) showed that the pyrrolopyridazine unit is more delocalized in **PC′** than in **PP′**. Thus, the N−N bond in **PC′** is shorter (1.343 Å) than in **PPH′** (1.361 Å) and in **PP′** (1.354 Å). The N═C bond in **PC′** is longer (1.333 Å) than in **PPH′** (1.299 Å) and in **PP′** (1.312 Å). The C(10a)═C(1) and C(2)═C(3) bonds in **PC′** are longer (1.404 Å and 1.398 Å) than in **PPH′** (1.388 Å and 1.382 Å) and in **PP′** (1.394 Å and 1.390 Å). The C(1)−C(2) bond in **PC′** is shorter (1.400 Å) than in **PPH′** (1.417 Å) and in **PP′** (1.409 Å).

A higher degree of delocalization requires contributions from both resonance structures **A** and **B**, leading to drawing **C**, which best describes the calculated structure of **PC′**. The significance of structure **B** results from a strong preference of the fused benzene ring to maintain maximum aromaticity. This leads to increased bond equalization in **PC′**, compared to that in **PP′** and **PPH′**, but also destabilizes it energetically. Calculations further revealed that the **PC** structure is less stable than **PPH** by 8.79 kcal/mol (at B3LYP/6-31G(d), corrected for unscaled zero-point energy differences (ZPVE)).

Benzannulation of **PP′** in the 3,4-positions produces **PPH′** (its analogue, **PPH** shows an unexpectedly shorter wavelength absorption of 319 nm, compared to **PP** (346 nm), despite the π-extension in **PPH**, Table 2). Analysis of the calculated geometries (Figure 6) showed that the pyrrolopyridazine unit is *less* delocalized in **PPH′** than in **PP′** and especially in **PC′**. Resonance structure **D** is a major contributor to the structure of **PPH′**, again due to strong tendency of the fused benzene ring to maintain aromaticity. Decreased delocalization (increased benzene localization) expectedly leads to absorption at shorter wavelength, although, in principle, **PPH** has a more extended π conjugation.

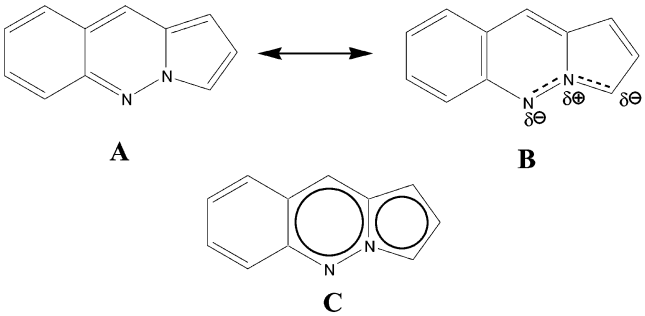

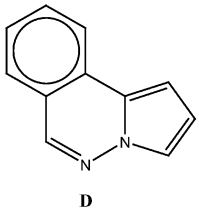

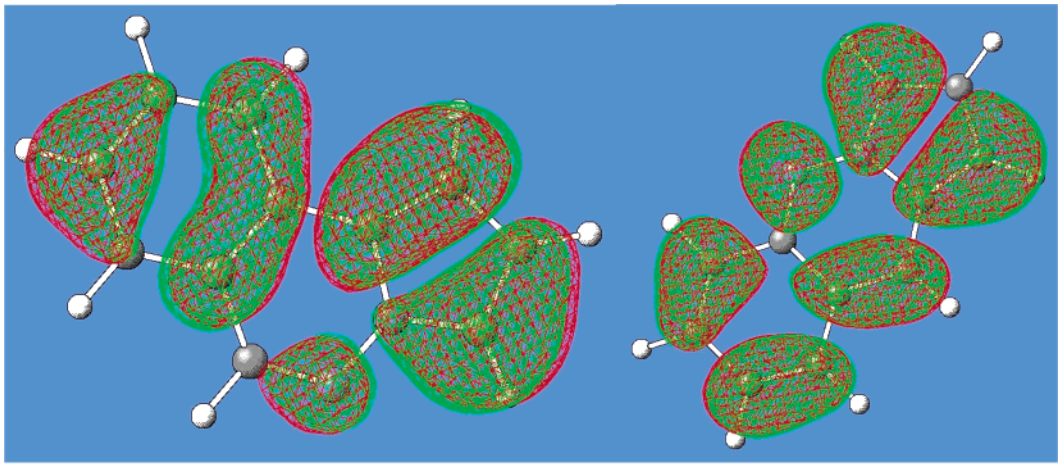

Figure 7. HOMOs of pyrrolopyridazines (**PPH′**, **PC′**) at the B3LYP/6-31G(d) level.

Table 3. Electrochemical Properties of 1, 4−6, 8−10, and PPY (Solvent:CH_3CN)

compd	**PPY**	**1**	**4**	**5**	**6**	**8**	**9**	**10**
Eox[a]	2.37/...[c]	1.92/...[c]	1.66/...[c]	1.56/1.38	1.35/...[c]	1.89/...[c]	1.63/...[c]	2.14/...[c]
Ered[b]	−2.04/...[c]	−1.21/−1.00	−1.14/−1.01	<−2.20[d]	−1.21/−1.36	−2.03/...[c]	<−2.20[d]	−1.68/−1.99

[a] Eox.pa/Eox.pc (V/SCE). [b] Ered.pa/Ered.pc (V/SCE). [c] Partially reversible. [d] Undetectable.

The structure of **PP** is intermediate between **PPH** and **PC**, which is consistent with its UV absorption (440 nm). Further differences in the electronic structure of **PPH′** and **PC′** can be found in the shapes of their HOMOs (Figure 7). The HOMO of **PC′** is delocalized over the whole aromatic system, while the HOMO of **PPH′** is localized on the benzene and pyrrole rings with smaller coefficients on the C═N bond of the pyridazine ring. The calculated HOMO−LUMO gap for **PPH′** and **PC′** (4.06 and 3.14 eV, respectively, at B3LYP/6-31G-(d)) is also consistent with the measured absorption spectra of **PPH** and **PC**.

Electrochemical Studies. Cyclic voltammetry (CV) is an important technique for measuring oxidation and reduction potentials, which are usually related to HOMO and LUMO energy levels, as well as for prediction of stability of optoelectronic devices. These values are important for rational designs of optoelectronic devices. Table 3 is a collection of electrochemical data for compounds **1**, **4**−**8**, **10**, and **PPY**.

Compared to **PPY** (ca. −2.4 V), **BPIDs** (**1**, **4**) have lower reduction potentials (from −1.6 to −1.9 V). This is due to the carbonyl groups that are in the molecular plane of **BPIDs**, whereas **PPY** has more bulky ester groups, which are out of plane. The quinone structure of **BPIDs** helped to stabilize the reduced state with the added feature of reversible redox. Interestingly, upon removal of the 11-carboxyl group, **BPID** (**4**) had lower oxidation potential than that of **BPID** (**1**) but its reduction potential remained unchanged. This indicates that the carbonyl at position 11 in **BPIDs** affects mainly the HOMO and the carbonyls at the 5,10-positions affect both the HOMO and LUMO. We can also extend this explanation to **PPs**.

Upon loss of a carboxyl group from position 7, the oxidation potential of **PP** (**8**) (1.9V) becomes much lower than that of **PPY** (2.4V), while the reduction potential remains unchanged (−2.0 V). In **PP** (**9**) both oxidation (1.6V) and reduction potentials (less than −2.2 V) are reduced, compared to **PP** (**8**) upon loss of the carboxyl group from position 5. This indicates that a carboxyl at position 7 affects the HOMO level but affects the LUMO level to a much lesser extent. These results are also explained by distribution of HOMO and LUMO levels. Frontier Orbital Theory[31] provides an explanation. The HOMO of the parent **PP′** has a large coefficient at position 7, so the substituent effect in this position on the oxidation potential is large (Figure 8). In contrast, the LUMO of **PP′** has a small coefficient at position 7, so the effect on the reduction potential by the substituent in this position is small (Figure 8).

As expected, compounds **5**, **6**, and **10** exhibit lower oxidation potentials (1.5, 1.5, and 2.1 V, respectively) than that of **PPY** (2.4V), very likely due to a longer π conjugation. Especially the oxidation potentials of fused ring compounds (**5** and **6**) are lowered by 0.9 V (to 1.5 V), compared to **PPY**. Unexpectedly, the relatively unstable compound **5** has a fully reversible CV in the oxidation process, which means the extended π system tends to stabilize cation radical species (the original **PPY** redox is partially reversible). The reduction potentials in **6** and **10** (−1.3 and −1.8 V) also changed relative to **PPY** (−2.0 V), attributable to stabilization of the radical anions by the extended π-system. This extended π-system also stabilizes the anion radicals kinetically and the reduction waves of **6** and **10** are fully reversible. This stability is very important for device applications.

The π-extension effect was especially large in **PC** (**6**), which also had an increased aromatic character by a fused ring. Auspiciously, the reduction and oxidation potentials of **PC** (**6**) are bracketed by conventional host

(31) Fleming, I. *Frontier Orbitals and Organic Chemical Reactions*; Wiley: New York, 1976.

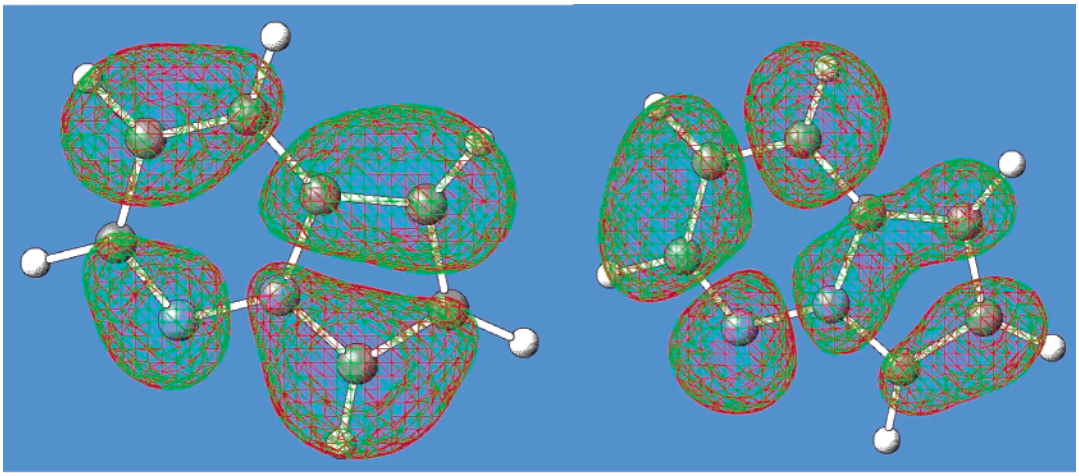

Figure 8. HOMO and LUMO of a pyrrolopyridazine (**PP′**) at the B3LYP/6-31G(d) level.

materials such as Alq_3 in OLED fabrication.[32] **PCs** have high luminescence, not only in solution but also in the solid state. They are therefore expected to be useful, not only as dopant as but also as host materials in luminescent devices and results of devices with **PCs** will be the subject of a future publication.

Conclusion

Ten new heterocycles, based on the pyrrolopyridazine unit, have been prepared and their optical and electronic properties, as well as their crystal structures, have been studied. These heterocycles have blue or green emission and their quantum efficiency was found to be very high, up to 90%. We also have shown the strategies by which HOMO−LUMO levels and emission colors were tunable without losing quantum efficiencies.

Especially important is the observation that **PCs** show remarkably large red shifts (about 100 nm) just by fusion of one phenylene unit, without loss in luminescence efficiency. Their HOMO−LUMO levels are ideal for device applications.[32] The large red shift in **PCs** was explained by bond length equalization arguments using DFT calculations and X-ray crystal structures.

Experimental Section

Synthesis of *N*-(*tert*-Butyloxycarbonylmethyl) Pyridazinium Bromide (S1). This compound was prepared according to the literature procedure.[6] Pyridazine (4.97 g, 62.0 mmol), *tert*-butyl bromoacetate (5.00 g, 62.0 mmol), and CH_2Cl_2 (100 mL) were charged in a 100-mL round-bottom flask equipped with a stirring bar. The mixture was refluxed for about 3 h under N_2 and a solid precipitated. The resulting mixture was cooled to room temperature and filtered under N_2. The solid was washed twice with CH_2Cl_2. *N*-(2-*tert*-Butyloxycalbonylmethyl) pyridazinium bromide (11.4 g, 40.3 mmol) was obtained as a pale orange crystalline solid. Yield 65%. mp 138 °C (decomp.). ^{1}H NMR (CD_3CN): δ 10.26−10.29 (m, 1H), 9.50−9.52 (m, 1H), 8.65−8.73 (m, 1H), 8.54−8.61 (m, 1H), 5.86 (s, 2H), 1.48 (s, 9H). ^{13}C NMR (CD_3CN): δ 163.6, 154.3, 151.3, 137.5, 135.7, 84.6, 65.0, 26.8. MS(EI+) *m*/*z*: 196.1 (MH^+−Br) . IR: ν (C═O) 1731 cm^{-1}.

11-*tert*-Butyloxycarbonyl Benzo[*f*]pyridazino[6,1-*a*]-isoindole-5,10-dione (1). This compound was prepared according to a modified literature procedure.[6,7] To a 200-mL round-bottom flask was added *N*-(*tert*-butyloxycarbonylmethyl) pyridazinium bromide (**S1**) (2.2 g, 8 mmol) and 1,4-naphthoquinone (4.64 g, 26 mmol) while stirring in CH_2Cl_2 (10 mL). A solution of NEt_3 (2.8 g, 28 mmol) in CH_2Cl_2 (5 mL) was added dropwise to give a black solution. After being stirred for 8 h, the solution was diluted with CH_2Cl_2 (50 mL), washed with H_2O (3 × 50 mL), and dried over anhydrous $MgSO_4$. The solvent was removed under reduced pressure to give a black oil. This oil was purified by column chromatography on silica gel with CH_2Cl_2. The fluorescent fractions were collected and isolated by solvent removal under reduced pressure. Recrystallization from CH_2Cl_2/hexane afforded a fine yellow solid (1.44 g, 4.13 mmol). Yield 52%. mp 215 °C (decomp). ^{1}H NMR ($CDCl_3$): δ 8.63 (dd, J = 1.9 Hz, 9.2 Hz), 8.56 (dd, J = 1.9 Hz, 4.5 Hz, 1H), 7.12 (dd, J = 4.5 Hz, 9.2 Hz, 1H), 4.00 (s, 3H), 3.91 (s, 3H), 1.60 (s, 9H). ^{13}C NMR ($CDCl_3$): δ 179.6, 178.0, 159.2, 146.3, 135.2, 135.0, 133.7, 133.3, 129.3, 129.1, 128.6, 127.2, 123.6, 122.5, 117.9, 110.5, 84.3, 28.1. MS(EI+) *m*/*z*: 348.1 (M^+). Elem. Anal. Calcd for $C_{20}H_{16}N_2O_4$: C, 68.96; H, 4.63; N, 8.04. Found: C, 68.76; H, 4.35; N, 7.93. IR: ν (C═O) 1705, 1679, 1645 cm^{-1}.

1-Methoxycarbonylmethyl Pyridazin-1-ium Iodide (S2). Chloroacetic acid methyl ester (25 g, 0.23 mol) was added to NaI (35.5 g, 0.237 mol) in dry acetone (300 mL) to form a yellow precipitate. Pyridazine (17.7 g, 0.221 mol) was then added, turning the suspension dark orange. The reaction was stirred for 20 min before the solid was collected by filtration. The product was washed with Et_2O to afford a pale brown solid (51.0 g, 0.182 mol). Yield 76.8%. mp 91−92.5 °C. ^{1}H NMR (CD_3CN): δ 10.00−10.06 (m, 1H), 9.50−9.55 (m, 1H), 8.67−8.75 (m, 1H), 8.59−8.66 (m, 1H), 5.86 (s, 2H), 3.79 (s, 3H). ^{13}C NMR (CD_3CN): δ 164.8, 154.2, 151.0, 137.6, 135.6, 64.5, 52.0. MS(EI+) *m*/*z*: 153.1 (M^+−I). IR: ν (C═O) 1744 cm^{-1}.

11-Methoxycarbonyl Benzo[*f*]pyridazino[6,1-*a*]isoindole-5,10-dione (2). This adduct was prepared by a similar procedure to compound **1**. To a 200-mL round-bottom flask was added 1-methoxycarbonylmethyl pyridazin-1-ium iodide (**S2**) (14 g, 50 mmol) and 1,4-naphthoquinone (19.4 g, 110 mmol) while stirring in CH_2Cl_2 (200 mL). A solution of NEt_3 (12.6 g, 125 mmol) in CH_2Cl_2 (50 mL) was added dropwise to give a black solution. After being stirred for 8 h, the solution was diluted with CH_2Cl_2 (200 mL), washed with H_2O (3 × 200 mL), and dried over anhydrous $MgSO_4$. The solvent was removed under reduced pressure to give a black oil. This oil was purified by column chromatography on alumina with CH_2Cl_2. The fluorescent fractions were collected and isolated by solvent

(32) (a) Posch, P.; Thelakkat, M.; Schmidt, H. W. *Synth. Met.* **1999**, *102*, 1110. (b) Kim, J.; Kim, E.; Choi, J. *J. Appl. Phys.* **2002**, *91*, 1944. (c) Lee, S. T.; Hou, X. Y.; Mason, M. G.; Tang, C. W. *J. Appl. Phys.* **1998**, *72*, 1593. (d) Vestweber, H.; Bassler, H. *J. Appl. Phys.* **2001**, *89*, 3711.

removal under reduced pressure. Recrystallization from CH_2Cl_2/hexane afforded a fine yellow solid (4.6 g, 15 mmol). Yield 30%. mp 230.5−231.3 °C. ^{1}H NMR ($CDCl_3$): δ 8.77 (dd, J = 1.9, 9.3 Hz, 1H), 8.49 (dd, J = 1.9, 4.5 Hz, 1H), 8.25 (dd, J = 4.9, 1.9 Hz, 2H), 7.75 (td, J = 4.9, 1.9 Hz, 2H), 7.17 (dd, J = 9.3, 4.5 Hz, 1H), 4.14 (s, 3H). ^{13}C NMR ($CDCl_3$): δ 180.0, 179.5, 160.6, 146.5, 135.1, 134.8, 133.9, 133.5, 129.4, 129.1, 127.3, 126.7, 123.5, 120.8, 118.2, 110.9, 53.3. MS(EI+) *m*/*z*: 306.1 (M^+). Elem. Anal. Calcd for $C_{17}H_{10}N_2O_4$: C, 66.67; H, 3.29; N, 9.15. Found: C, 67.00; H, 3.08; N, 9.09. IR: ν (C═O) 1727, 1680, 1653 cm^{-1}.

1-(2-Oxo-propyl) Pyridazin-1-ium Iodide (S3). Chloroacetone (12 g, 130 mmol) was added to NaI (20.0 g, 133 mmol) in 200 mL of dry acetone to form a yellow precipitate. Pyridazine (10.0 g, 125 mmol) was then added, turning the suspension orange. The reaction was stirred for 20 min before the solid was collected by filtration. The product was washed with Et_2O to give an iodide salt (15.8 g, 60 mmol). Yield 48%. mp 162 °C. ^{1}H NMR (CD_3CN): δ 9.70−9.72 (m, 1H), 9.46−9.48 (m, 1H), 8.62−8.68 (m, 1H), 8.52−8.56 (m, 1H), 6.00 (s, 2h), 2.37 (s, 3H). ^{13}C NMR (CD_3CN): δ 197.3, 154.2, 150.6, 137.1, 135.4, 72.3, 26.7. MS(EI+) *m*/*z*: 136.1 as (MH^+−I). IR: ν (C═O) 1740 cm^{-1}.

11-Acetyl Benzo[*f*]pyridazino[6,1-*a*]isoindole-5,10-dione (3). This adduct was prepared by a similar procedure to compound **1**. To a 200-mL round-bottom flask was added 1-(2-oxo-propyl) pyridazin-1-ium iodide (**S3**) (13.2 g, 50 mmol) and 1,4-naphthoquinone (29.1 g, 165 mmol) while stirring in CH_2Cl_2 (200 mL). A solution of NEt_3 (17.7 g, 175 mmol) in CH_2Cl_2 (100 mL) was added dropwise to give a black solution. After being stirred for 8 h, the solution was diluted with CH_2Cl_2 (200 mL), washed with H_2O (3 × 200 mL), and dried over anhydrous $MgSO_4$. The solvent was removed under reduced pressure to give a black oil. This oil was purified by column chromatography on alumina with CH_2Cl_2. The fluorescent fractions were collected and isolated by solvent removal under reduced pressure. Recrystallization from CH_2Cl_2/hexane afforded a fine yellow solid (3.5 g, 15.5 mmol). Yield 31%. mp 216−216.5 °C. ^{1}H NMR ($CDCl_3$): δ 8.81 (dd, J = 9.5, 2.0 Hz, 1H), 8.49 (dd, J = 2.0, 4.6 Hz, 1H), 8.30−8.25 (m, 2H), 7.80−7.74 (m, 2H), 7.18 (dd, J = 9.5, 4.6 Hz, 1H), 2.92 (s,3H). ^{13}C NMR ($CDCl_3$): δ 192.9, 180.8, 179.6, 146.5, 135.0, 134.8, 134.0, 133.5, 129.5, 129.3, 128.1, 127.4, 126.6. 123.1, 118.4, 110.8, 31.6. MS(EI+) *m*/*z*: 290.1 (M^+). Elem. Anal. Calcd for $C_{17}H_{10}N_2O_3$: C, 70.34; H, 3.47; N, 9.65. Found: C, 70.04; H, 3.24; N, 9.58. IR: ν (C═O) 1692, 1673, 1654 cm^{-1}.

Benzo[*f*]pyridazino[6,1-*a*]isoindole-5,10-dione (4). This compound was prepared by decarboxylation (a modified literature procedure)[8] of compound **1**. 11-*tert*-Butyloxycarbonyl benzo[*f*]pyridazino[6,1-*a*]isoindole-5,10-dione (**1**) (50 mg, 0.14 mmol) was dissolved in dry acetone (30 mL) and hydroiodic acid (45% aqueous solution) (6 mL) was added dropwise under Ar.[8] The color of the mixture changed gradually from yellow to red. After 8 h of stirring at reflux, the reaction mixture was washed with aqueous $NaHSO_3$ (3 × 50 mL), with H_2O (2 × 50 mL), and dried over anhydrous $MgSO_4$. The solvent was removed under reduced pressure to give a brown oil. This oil was purified by column chromatography on silica gel with CH_2Cl_2. All fluorescent fractions were collected and isolated by solvent removal under reduced pressure. Recrystallization from CH_2Cl_2/hexane afforded a fine yellow solid (25 mg, 0.10 mmol). Yield 71%. mp 227.3−228.5 °C. ^{1}H NMR ($CDCl_3$): δ 8.67 (dd, J = 9.1, 1.8 Hz, 1H), 8.36 (ddd, J = 4.4, 1.8, 0.5 Hz, 1H), 8.29 (d, J = 7.4 Hz, 1H), 8.25 (d, J = 0.5 Hz, 1H), 7.76 (dd, J = 7.4, 15.5 Hz, 1H), 7.74 (dd, J = 7.4, 15.5 Hz, 1H), 7.06 (dd, J = 9.1, 4.4 Hz, 1H). ^{13}C NMR ($CDCl_3$): δ 181.4, 179.4, 146.0, 135.9, 134.8, 133.8, 133.1, 129.3, 129.1, 129.0, 127.1, 126.8, 124.6, 118.8, 117.2. MS(EI+) *m*/*z*: 248.1 (M^+). Elem. Anal. Calcd for $C_{15}H_8N_2O_2$: C, 72.58; H, 3.25; N, 11.29. Found: C, 72.28; H, 2.98; N, 11.20. IR: ν (C═O) 1672, 1658 cm^{-1}.

5,10-Dimethoxyl Benzo[*f*]pyridazino[6,1-*a*]isoindole (5). Benzophenone (307 mg, 1.68 mmol) and Na (38.7 mg, 1.68 mmol) were charged in a 100-mL round-bottom flask under N_2. Distilled THF (10 mL) was added and the solution was stirred for 1.5 h. The mixture turned from blue to dark blue.[10] To this solution benzo[*f*]pyridazino[6,1-*a*]isoindole-5,10-dione (**4**) (190 mg, 0.765 mmol) in distilled THF (30 mL) was added at −73 °C. The color changed to dark purple. After the solution was stirred for 24 h, ether (50 mL) was added and the mixture was washed with aqueous NH_4Cl (2 × 50 mL), with H_2O (50 mL), and dried with $MgSO_4$. The solvent was removed under reduced pressure to give a brown oil. This oil was purified by column chromatography on silica gel with hexane/ethyl acetate = 4/1 → 3/1. All fluorescent fractions were collected and isolated by solvent removal under reduced pressure to afford a yellow solid (80 mg, 0.287 mmol). Yield 37%. mp 85 °C (decomp). ^{1}H NMR ($CDCl_3$): δ 8.77 (dd, J = 9.0, 1.8 Hz, 1H), 8.39 (t, J = 3.9 Hz, 1H), 8.30 (dd, J = 4.5, 1.8 Hz, 1H), 7.85 (s, 1H), 7.78(d, J = 3.9 Hz, 1H), 7.66 (t, J = 3.9 Hz, 1H), 7.51 (t, J = 3.9 Hz, 1H), 7.00 (dd, J = 9.0, 4.5 Hz, 1H), 2.90 (s, 3H), 1.84 (s, 3H). ^{13}C NMR ($CDCl_3$): δ 147.8, 144.2, 134.8, 133.5, 132.9, 129.1, 128.2, 128.0, 126.6, 126.5, 118.8, 117.6, 117.5, 115.0, 110.2, 52.3, 35.2. HRMS: found, 278.1053; calcd for $C_{17}H_{14}N_2O_2$ 278.1055.

Pyrrolo[1,2-b]cinnoline-1,2,3-tricarboxylic acid Trimethyl Ester (6). This compound was prepared according to a modified literature procedure[6,8] via a one-step reaction. Cinnoline hydrochloride hydrate (500 mg) was dispersed in distilled CH_2Cl_2 (5 mL). A solution of NaOH (216 mg) in H_2O (3 mL) was added and the mixture was mixed gently. The solution turned green. The organic layer was washed with H_2O (2 × 2 mL) and dried over $MgSO_4$ and the solvent was evaporated to leave a green oil (400 mg, 3.08 mmol). The residue was dissolved in MeOH and stirred at −5 °C. To this mixture dimethyl acetylenedicarboxylate (**DMAD**) (3 mL) was added dropwise over 10 min. The color changed to red and at last to black. The mixture was stirred for 12 h at room temperature, followed by dilution with CH_2Cl_2 to 50 mL. The organic phase was washed once with 20 mL of water and dried over $MgSO_4$. The solvents were removed with a rotary evaporator, and a black semisolid mixture was obtained. The residue was purified by chromatography on SiO_2 (500 g) with ethyl acetate:hexane = 2:1 and recrystallized from CH_2Cl_2 and hexane to obtain a yellow solid (45 mg, 0.13 mmol). Yield 4.3%. mp 130.0−131.5 °C. ^{1}H NMR ($CDCl_3$): δ 9.22 (s, 1H), 8.07 (dd, J = 0.4, 4.7 Hz, 1H), 7.81 (dd, J = 4.0, 0.4 Hz, 1H), 7.68 (dd, J = 4.0, 4.7 Hz, 1H), 7.47 (td, J = 4.0, 0.4 Hz, 1H), 4.06 (s, 3H), 4.01 (s, 3H), 3.98 (s, 3H). ^{13}C NMR ($CDCl_3$): 165.8, 162.8, 158.9, 147.8, 146.7, 132.1, 131.8, 129.1, 128.1, 127.2, 126.6, 126.3, 122.6, 101.2, 53.1, 52.2, 52.0. MS(FAB+) *m*/*z*: 342.1 (M^+). Elem. Anal. Calcd for $C_{17}H_{14}N_2O_6$: C, 59.65; H, 4.12; N, 8.18. Found: C, 59.40; H, 4.20; N, 8.10. IR: ν (C═O) 1741, 1701, 1684 cm^{-1}.

2-*tert*-Butoxycarbonylmethyl Cinnolin-2-ium Bromide (S4). Cinnoline hydrochloride hydrate (1.00 g) was dispersed in distilled CH_2Cl_2 (5 mL). A solution of NaOH (216 mg) in H_2O (3 mL) was added and the mixture was mixed gently. The solution turned green. The organic layer was washed with H_2O (2 × 2 mL) and dried over $MgSO_4$. The solvent was evaporated and the residue was dried in vacuo to obtain cinnoline (750 mg, 5.78 mmol). The cinnoline and CH_2Cl_2 (30 mL) were charged in a 100-mL round-bottom flask equipped with a stirring bar. To the solution bromoacetic acid *tert*-butyl ester (1.15 g, 5.92 mmol) was added. The mixture was refluxed for 3 h under N_2 and a solid precipitated. The resulting mixture was cooled to room temperature and hexane (50 mL) was added and the precipitate was filtered under N_2. The solid was washed with hexane (2 × 20 mL) and dried in vacuo for 6 h to afford a mixture of 1,2-position isomers (750 mg, 2.31 mmol). The ratio of 1- and 2-position isomers was 3:7**.** *1-tert-Butoxycarbonylmethyl cinnolin-1-ium bromide.* ^{1}H NMR (CD_3CN): δ 9.40 (d, J = 6.0 Hz, 1H), 9.17 (d, J = 6.0 Hz, 1H), 8.79−8.76 (m, 1H), (m, 1H), 8.3−8.2 (m, 3H), 1.48 (s, 9H). Yield 12%. *2-tert-Butoxycarbonylmethyl cinnolin-2-ium bromide.* ^{1}H NMR (CD_3CN): δ 9.72 (d, J = 6.5 Hz, 1H), 9.17 (d, J = 6.5 Hz, 1H), 8.55−8.47 (m, 1H), 8.45−8.39 (m, 1H), 8.38−8.29 (m, 2H), 5.93 (s, 1H), 1.48 (s, 9H). Yield 28%. MS(FAB+) *m*/*z*: 245.1 ($M-Br)^+$.

Pyrrolo[1,2-b]cinnoline-1,2,3-tricarboxylic Acid 3-*tert*-Butyl Ester 1,2-Dimethyl Ester (7). This adduct was prepared by a similar procedure to compound **1**. To a 50-mL round-bottom flask was added a mixture of *tert*-butoxycarbonylmethyl cinnolinium bromides (**S4**) (700 mg, 2.16 mmol) and **DMAD** (1.23 g, 8.7 mmol), while stirring in CH_2Cl_2 (20 mL). The green solution was brought to reflux. A solution of NEt_3 (0.404 g) in CH_2Cl_2 (5 mL) was added dropwise. The color changed from green to brown. The solution was refluxed for 12 h. The solution was diluted with CH_2Cl_2 (10 mL), washed with H_2O (2 × 5 mL), and dried over $MgSO_4$. The solvent was evaporated in vacuo to leave a black oil. The residue was chromatographed on silica gel (500 g) with hexane:ethyl acetate = 2:1 to obtain a yellow solid (60 mg, 0.16 mmol). Yield 7.6%. mp 130.0−131.5 °C. ^{1}H NMR ($CDCl_3$): δ 9.19 (s, 1H), 8.08 (d, J = 4.6 Hz, 1H), 7.79 (dd, J = 4.0, 0.5 Hz, 1H), 7.65 (ddd, J = 4.0, 4.6, 0.5 Hz, 1H), 7.44 (td, J = 4.0 Hz, 1H), 4.04 (s, 3H), 3.97 (s, 3H), 1.64 (s, 9H). ^{13}C NMR ($CDCl_3$): δ 165.8, 162.9, 157.5, 146.7, 132.0, 131.5, 129.1, 127.9, 127.2, 126.7, 126.1, 122.4, 120.0, 100.9, 82.7, 52.9, 51.9, 28.3. MS(EI+) *m/z*: 384.1 (M^+). Elem. Anal. Calcd for $C_{20}H_{20}N_2O_6$: C, 62.49; H, 5.24; N, 7.29. Found: C, 62.60; H, 5.20; N, 7.20. IR: ν (C=O) 1737, 1725, 1700 cm^{-1}.

Pyrrolo[1,2-b]pyridazine-5,6-dicarboxylic Acid Dimethyl Ester (8). Pyrrolo[1,2-b]pyridazine-5,6,7-tricarboxylic acid 7-*tert*-butyl ester 5,6-dimethyl ester **11** (prepared according to the literature procedure)[6] (100 mg, 0.29 mmol) and distilled $ClCH_2CH_2Cl$ (20 mL) were charged into a 50-mL round-bottom flask at 0 °C under N_2. Trifluoroacetic acid (TFA) (132 mg, 1.16 mmol) was added dropwise and the mixture was allowed to warm to r.t. The reaction mixture was stirred for 1 h (until there was no trace of *tert*-butyl ester), followed by warming up to 60 °C with stirring for 30 h. The mixture was washed with aqueous $NaHCO_3$ (50 mL), with H_2O (50 mL), and dried over $MgSO_4$. The extracts were evaporated to leave a yellow-brown viscous residue. The residue was chromatographed on silica gel three times with hexane:ethyl acetate = 4:1 → 3:1. The solid was recrystallized from CH_2Cl_2 and hexane. The precipitate was collected and dried to afford a white solid, 38 mg (0.16 mmol). Yield 55%. mp 67.5−69.0 °C. ^{1}H NMR ($CDCl_3$): δ 8.43 (ddd, J = 4.8, 0.3, 0.9 Hz 1H), 8.22 (dd, J = 2.3, 0.9 Hz, 1H), 8.04 (dd, J = 4.8, 0.3 Hz, 1H), 3.93 (s, 3H), 3.92 (s, 3H). ^{13}C NMR ($CDCl_3$): δ 164.5, 163.6, 144.5, 129.9, 128.8, 121.2, 120.1, 115.2, 103.6, 52.3, 51.6. MS(EI+) *m/z*: 234.1 (M^+). Elem. Anal. Calcd for $C_{11}H_{10}N_2O_4$: C, 56.41; H, 4.30; N, 11.96. Found: C, 56.35; H, 4.32; N, 11.76. IR: ν (C=O) 1736, 1679 cm^{-1}.

Pyrrolo[1,2-b]pyridazine-6-carboxylic Acid Methyl Ester (9). In a 200-mL round-bottom flask, pyrrolo[1,2-b]-pyridazine-5,6,7-tricarboxylic acid 7-*tert*-butyl ester 5,6-dimethyl ester (668 mg, 2.86 mmol) was dissolved in acetone (100 mL). Hydroiodic acid (45% aqueous solution) (2 mL) was added to this solution. The mixture was refluxed for 30 h, whereupon the color changed gradually from dark yellow to red. A 50-mL portion of MeOH was added and the reaction was refluxed for 30 h. The mixture was washed with H_2O (2 × 50 mL), with aqueous Na_2CO_3 (50 mL), and dried over $MgSO_4$, followed by evaporation of the solvent and the crude was purified using chromatography (SiO_2) with hexane:ethyl acetate = 4:1 → 2:1 and recrystallized from the hexane:CH_2Cl_2 system to afford a pale yellow solid (160 mg, 0.91 mmol). Yield 32%. mp 95−96.5 °C. ^{1}H NMR ($CDCl_3$): δ 8.19 (d, J = 1.7 Hz, 1H), 8.06 (dd, J = 4.4, 1.9 Hz, 1H), 7.73 (dd, J = 9.3, 1.7 Hz, 1H), 6.92 (d, J = 1.7 Hz, 1H), 6.55 (dd, J = 9.3, 4.4 Hz, 1H), 3.90 (s, 3H). ^{13}C NMR ($CDCl_3$): δ 165.1, 144.0, 128.5, 126.6, 120.0, 118.5, 111.0, 101.2, 51.6. HRMS *m/z*: found, 176.0580; calcd for $C_9H_8N_2O_2$, 176.0585. Elem. Anal. Calcd for $C_9H_8N_2O_2$: C, 61.36; H, 4.58; N, 15.90. Found: C, 61.37; H, 4.54; N, 15.95. IR: ν (C=O) 1706 cm^{-1}.

2-Phenyl-pyrrolo[1,2-b]pyridazine-5,6,7-tricarboxylic Acid Trimethyl Ester (10). This adduct was prepared by a similar procedure to compound **6**. First, 3-phenyl-pyridazine (prepared according to the literature procedures)[11] (1.56 g, 10 mmol) and dry MeOH (15 mL) in dry CH_2Cl_2 (10 mL) were placed in a 50-mL round-bottom flask equipped with a stirring bar. To this mixture, which was cooled to −5 °C, **DMAD** (1.7 mL) was added in several portions. The solution was stirred for 7 h at room temperature, whereupon a solid began to precipitate. The mixture was placed in a refrigerator overnight, followed by filtration, affording a pale yellow solid. The crude was chromatographed on silica gel (300 g) and eluted with hexane:ethyl acetate = 2:1 and the main fluorescent fraction was collected and isolated by solvent removal under reduced pressure. The white solid was recrystallized from CH_2Cl_2 and hexane. The precipitate was collected and dried to afford a white solid (800 mg, 2.17 mmol). Yield 22%. mp 256.0−256.5 °C. ^{1}H NMR ($CDCl_3$): δ 8.64 (d, J = 9.5 Hz, 1H), 8.10−8.05 (dd, 2H), 7.61 (d, J = 9.5 Hz, 1H), 7.55−7.48 (m, 3H), 4.02 (s, 3H), 3.98 (s, 3H), 3.92 (s, 3H). ^{13}C NMR ($CDCl_3$): δ 165.7, 162.8, 158.8, 153.2, 134.8, 130.8 130.7, 129.2, 128.8, 128.3, 127.2, 117.5, 116.5, 102.7, 53.0, 52.2, 51.9. HRMS: found, 368.1002; calcd for $C_{19}H_{16}N_2O_6$, 368.1008. Elem. Anal. Calcd for $C_{19}H_{16}N_2O_6$: C, 61.95; H, 4.38; N, 7.61. Found: C, 62.18; H, 4.53; N, 7.65. IR: ν (C=O) 1699, 1752, 1745 cm^{-1}.

Cyclic Voltammetry (CV) Measurement. Cyclic voltammetry was performed with a three-electrode cell in an acetonitrile solution of 0.1 M tetrabutylammonium hexafluorophosphate (Bu_4NPF_6) at a scan rate of 100 mV/s. A Pt wire was used as a counter electrode, glassy carbon was used as a working electrode, and an $Ag/AgNO_3$ (0.1 M) electrode was used as a reference electrode. Its potential was corrected to the saturated calomel electrode (SCE) by measuring the ferrocene/ferrocenium couple in this system (0.44 V versus SCE).[33]

X-ray Crystal Structure. Diffraction data were collected at low temperature (100 K) with graphite-monochromatized Mo Kα radiation (λ = 0.71073 Å). The cell parameters were obtained from the least-squares refinement of the spots using the SMART program. The structures were solved by direct methods using SHELXS-97, which revealed the positions of all non-hydrogen atoms. This was followed by several cycles of full-matrix least-squares refinement. Absorption corrections were applied by using SADABS.[34] Hydrogen atoms were included as fixed contributors to the final refinement cycles. The position of hydrogen atoms were calculated on the basis of idealized geometry. In the final refinement, all non-hydrogen atoms were refined with anisotropic thermal coefficients.

Acknowledgment. We are grateful to Dr. S. I. Khan for X-ray crystallographic analysis (Department of Chemistry and Biochemistry, UCLA). We are grateful to Mitsubishi Chemical Corporation for support of T.M. We also thank the ONR for support through Grant N00014-97-1-0835 and to National Computational Science Alliance for computational time (CHE020016N).

Supporting Information Available: General experimental procedure, crystal data, atomic coordinates, bond length, bond angles, anisotropic displacement parameters, hydrogen coordinates, isotropic displacement parameters, torsion angles, and ORTEP diagrams for **PPH**, **PP (8)**, and **PC (7)**. Absolute energies and optimized geometries (in Cartesian coordinates) for all calculated compounds at B3LYP/6-31G(d). Absorption and fluorescence spectra of compounds **4**−**10** and **PPY** (PDF and CIF). This material is available free of charge via the Internet at http://pubs.acs.org.

CM0340532

(33) Clerac, R.; Cotton, F. A.; Dunbar, K. R.; Lu, T.; Murillo, C. A.; Wang, X. *J. Am. Chem. Soc.* **2000**, *122*, 2272.
(34) Blessing, R. H. *Acta Crystallogr.* **1995**, *A51*, 33.